

# MALDI QUADRUPOLE ORTHOGONAL ACCELERATION-TOF MASS SPECTROMETRY ENHANCED WITH ION MOBILITY SPECTROMETRY FOR TISSUE IMAGING

Waters  
THE SCIENCE OF WHAT'S POSSIBLE.™

<sup>1</sup>Marten F Snel, <sup>2</sup>Paul J Trim, <sup>1</sup>Emmanuelle Claude, <sup>1</sup>Thérèse McKenna, <sup>1</sup>James I Langridge  
<sup>1</sup> Waters Corporation, Manchester, UK; <sup>2</sup> Sheffield Hallam University, Sheffield, UK

## INTRODUCTION

A major limitation of MALDI MS imaging using conventional MALDI ToF and ToF-ToF analysers, which separate by  $m/z$ , is the absence of any additional dimension of separation. Due to the complexity of the samples under investigation, there is a risk of isobaric ions distorting the ion distribution and thus invalidating results.

With the MALDI SYNAPT HDMS system, it is possible to separate ions using ion mobility separation (IMS) prior to mass analysis. IMS separates ions according to their size, shape and charge state. Using this technique it is possible to separate different compound classes, giving additional confidence that the true distribution of an ion of interest is observed.

Here we use high efficiency ion mobility separations based on travelling wave (T-wave) technology<sup>1</sup> incorporated into the mass spectrometer. TriWave consists of three T-wave devices (see Figure 1). The first T-wave (Trap) is used to trap ions during the period when an IMS separation is being performed in the second T-Wave, thus greatly enhancing the efficiency of the IMS process. The final T-wave (Transfer) transports the separated ions to the TOF analyser. In addition fragmentation experiments can be performed in either or both the Trap and Transfer T-Wave regions e.g. providing Transfer fragmentation of two isobaric species that have been separated by their ion mobilities.

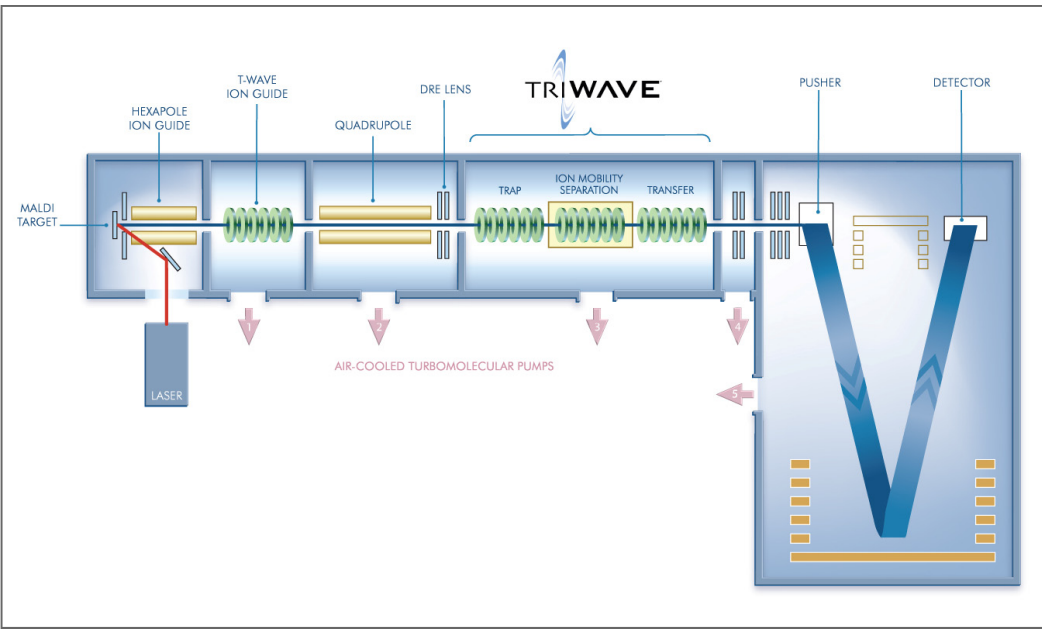


Figure 1. Schematic of the MALDI Synapt HDMS system, showing the TriWave Ion Mobility Separation device.

## METHODS

The sample under investigation was a thin section of rat kidney. A 12  $\mu\text{m}$  section was produced using a cryotome and deposited on thick aluminium foil.  $\alpha$ -cyano-4-hydroxycinnamic acid (CHCA) matrix was applied evenly to the sample in several coats using an airbrush. The sample was mounted on a target plate.

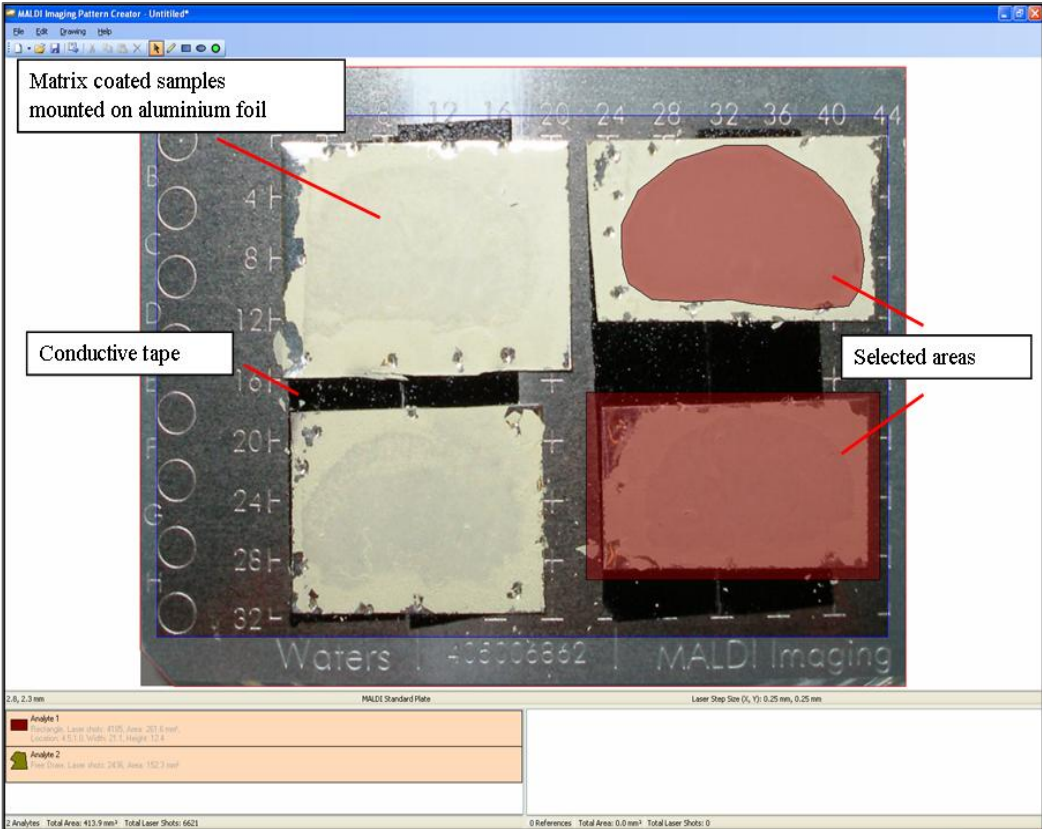


Figure 2. MALDI Imaging Pattern Creator is used to select area(s) to be automatically imaged using MALDI SYNAPT HDMS.

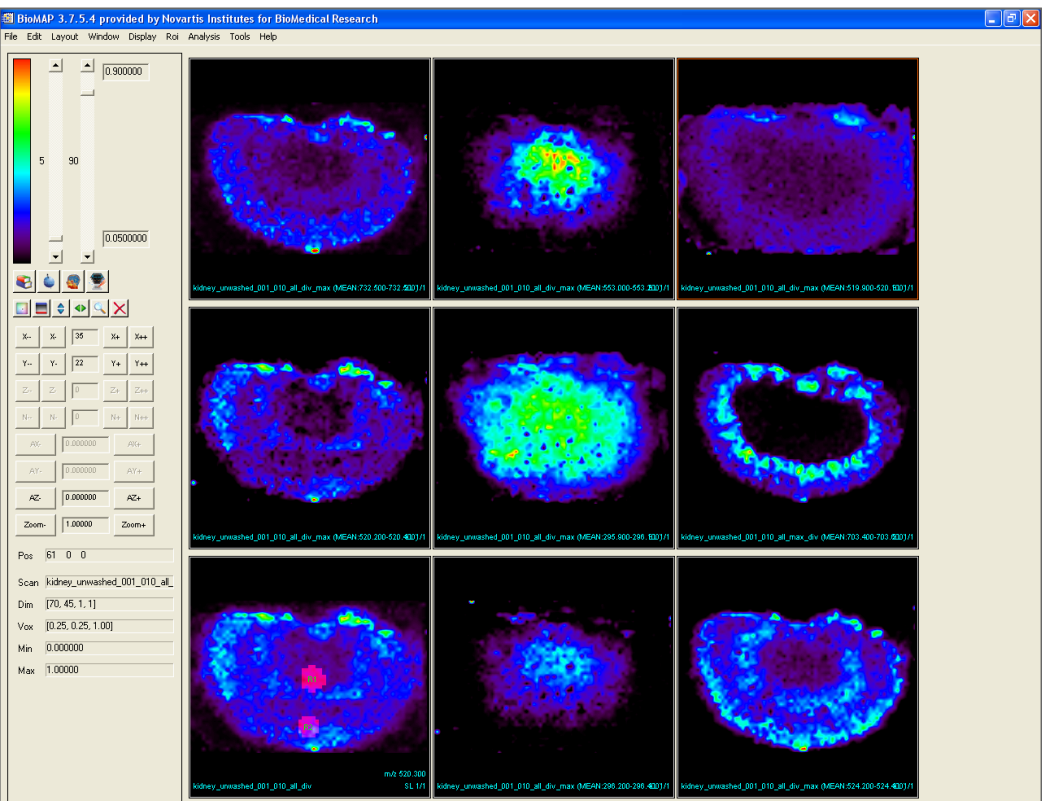


Figure 3. Illustration of image analysis of the kidney section using BioMap.

The area to be imaged was selected using MALDI Imaging Pattern Creator (Waters Corporation, Manchester, UK) (see Figure 2). Data were acquired on a MALDI Synapt HDMS system (Waters Corporation, Manchester, UK) operated in HDMS mode over the  $m/z$  range of 10 to 1000. Spatial resolution of 250  $\mu\text{m}$  was selected and 600 laser shots were acquired per pixel at a laser repetition rate of 200 Hz. After acquisition HDMS data evaluation was performed using Driftscope (Waters Corporation, Manchester, UK). Data were converted into Analyze file format using MALDI Imaging Converter (Waters Corporation, Manchester, UK) for image analysis using BioMap (Novartis, Basel, CH) (see Figure 3).

## RESULTS

### MS only MALDI imaging

The mass spectral data obtained during imaging experiments are often very complex, as is illustrated in Figure 4. This can often lead to the situation where two or more isobaric species are present. It can be seen from the mass spectrum shown in Figure 5 that two peaks with a nominal mass of 402 Da partially overlap, the larger of the two peaks (402.079 Da) was identified as the <sup>13</sup>C isotope of the sodiated dimer of CHCA, the other species (402.019 Da) could not be identified. Ion intensity maps were generated for both ions which show different distribution. (Figure 6). The higher intensity signal from the 402.019 Da species was observed in the centre of the kidney, however a strong signal was also observed outside the tissue (Fig. 6 (a)). The unexpected signal outside the tissue is attributable to interference from the larger peak at 402.079. The distribution of the sodiated matrix dimer ion is typical of matrix ions, with the highest intensity observed off tissue and reduced intensity on tissue, due to ionisation suppression effects on the tissue from salts and competing ions.

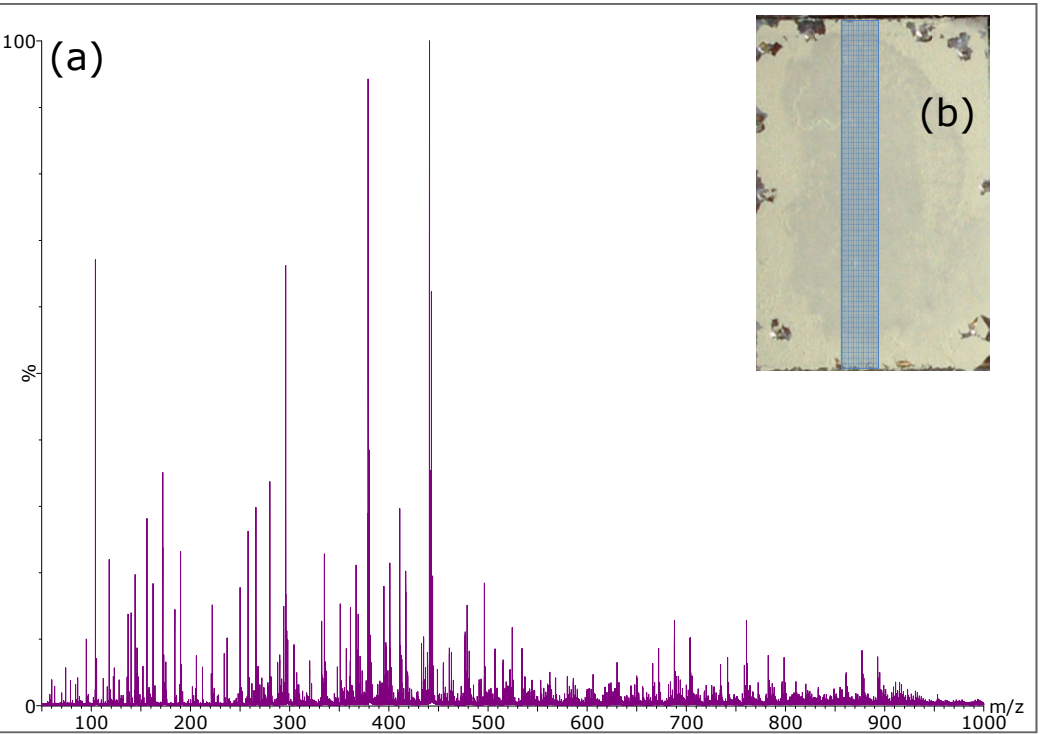


Figure 4. (a) combined mass spectrum averaged across the area of tissue highlighted in blue in (b) photo of matrix coated kidney sample.

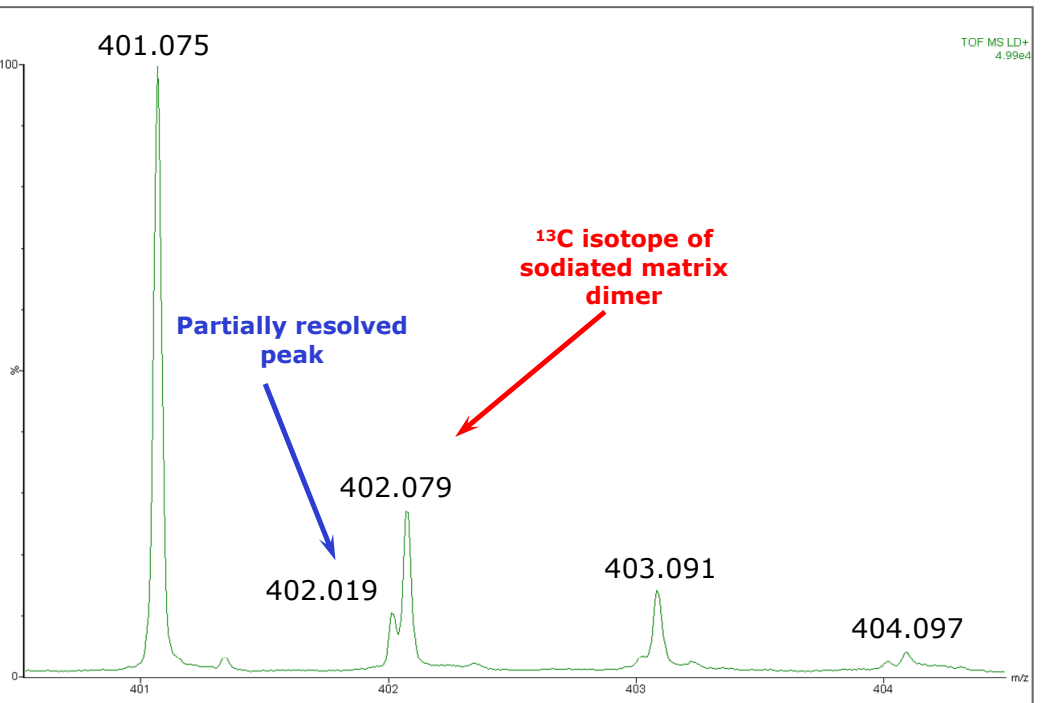


Figure 5. Partially overlapping peaks observed in an imaging experiment. This is a common occurrence owing to sample complexity.

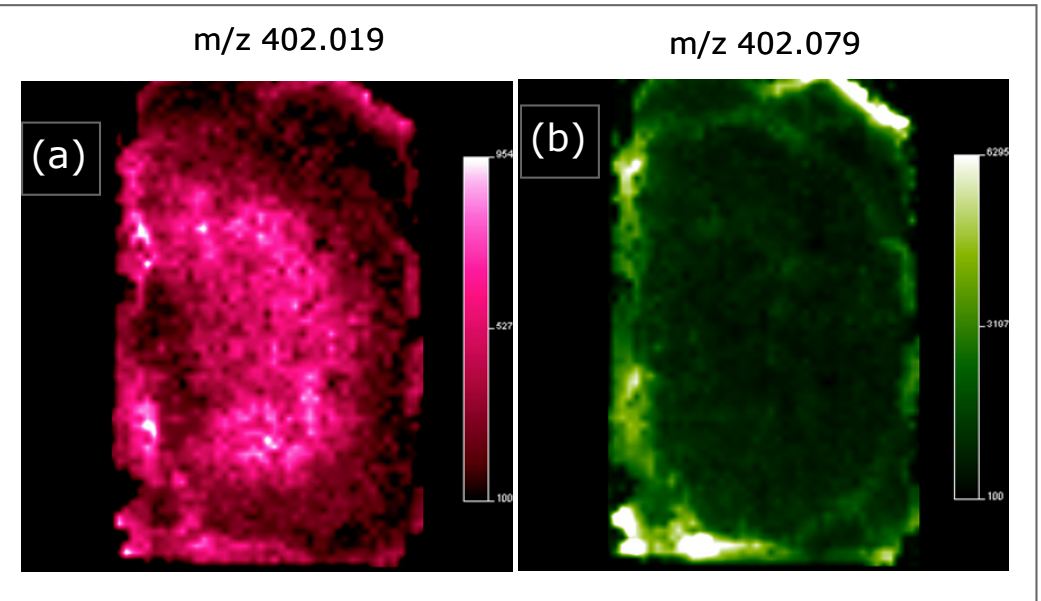


Figure 6. Ion intensity images for (a) the ion with  $m/z$  402.019 Da and (b) the <sup>13</sup>C isotope of sodiated CHCA dimer (402.079 Da)

### MALDI IMS imaging

The use of IMS adds a further dimension of separation occurring post ionization, and as such lends itself to coupling with a MALDI imaging experiment,

The combined Driftscope mobility plot showing drift time (x-axis) vs  $m/z$  (y-axis) obtained from the kidney sample is shown in Figure 7. It can clearly be seen that ions of similar  $m/z$  i.e. those on the same horizontal line in the plot, are separated in the ion mobility dimension. The region around  $m/z$  402 is enlarged and it can be observed that the ions discussed previously are separated in the ion mobility dimension. A full 3D data set consisting of  $m/z$ , IMS and intensity is acquired at every spatial position. This provides maximum flexibility for mining the data. It is also possible to perform a targeted experiment where only a small mobility and/or  $m/z$  range is acquired (not shown here).

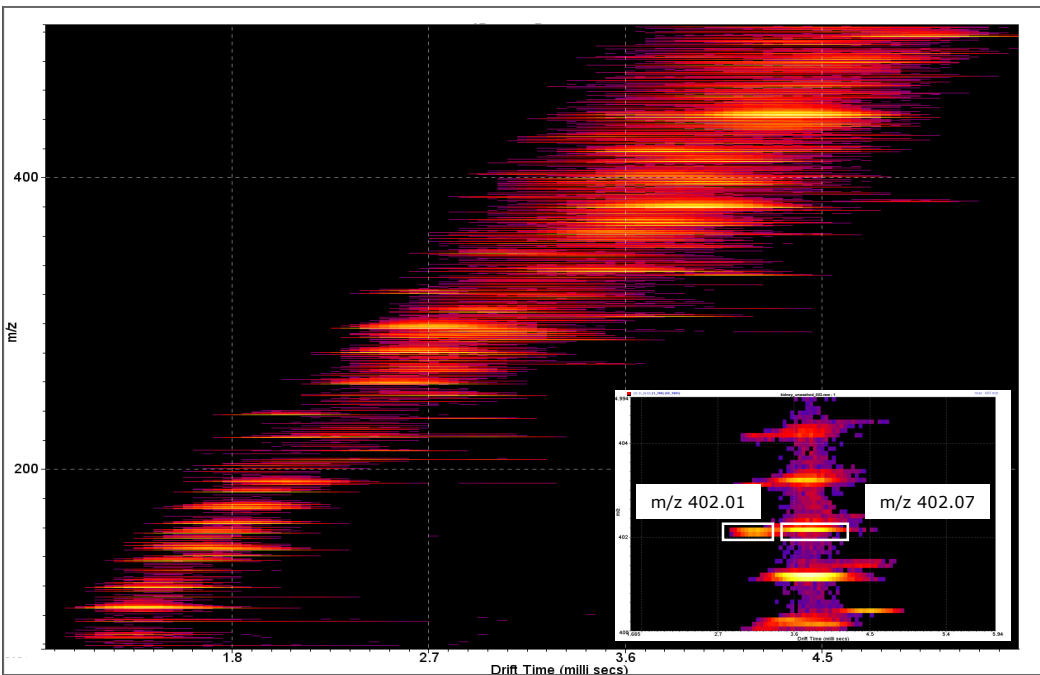


Figure 7. DriftScope data plot combined across the entire tissue section. Inset shows region ( $m/z$  400.5 – 405, IMS 2.3ms – 5.0ms).

Exact mass drift time chromatograms of the 402.019 Da and 402.079 Da show the separation of the two species (Figure 8), when mass spectra are produced for the indicated drift times, 2.7 ms – 3.3 ms and 3.4 ms – 4.1 ms respectively, almost complete separation is achieved.

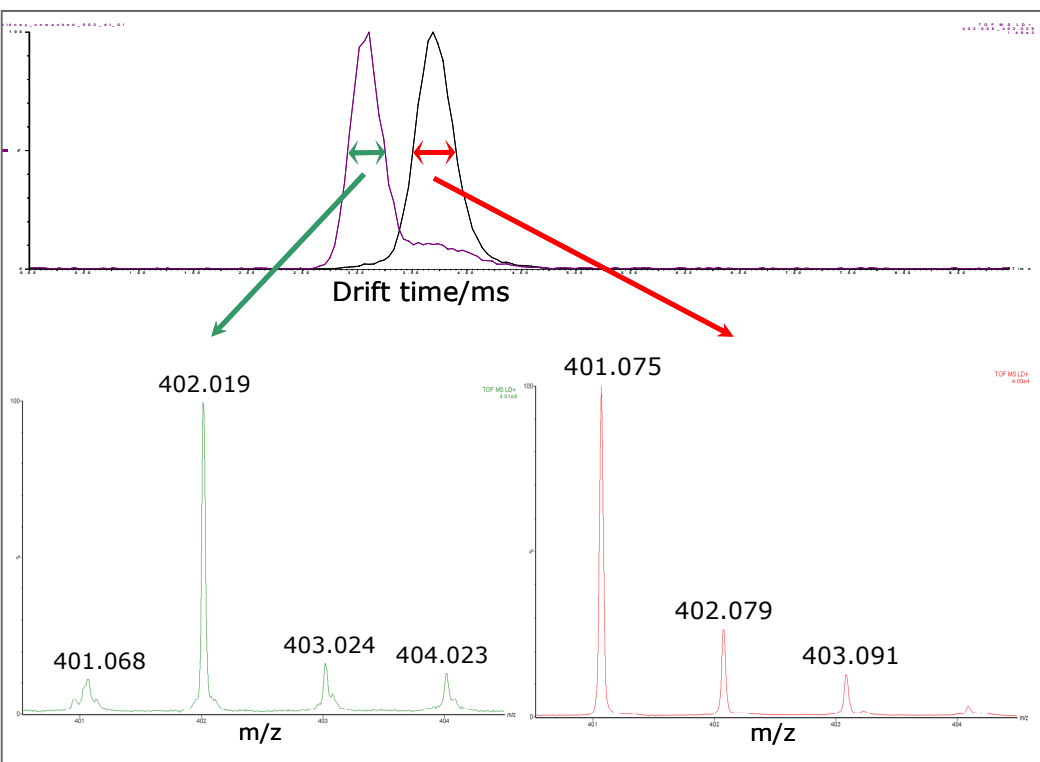


Figure 8. Separation of two isobaric ions based on their ion mobility. Top: Exact mass drift time chromatograms for  $m/z$  402.019 and 402.079, bottom: mass spectra from selected IMS regions show effective separation.

When selected drift times are used for generating ion images of these isobaric components, distinctly different images are produced. After ion mobility separation, the ion intensity of the 402.019 Da ion, Figure 9(a), is localised in the centre of the tissue with very little intensity outside the tissue showing that it was possible to remove the interfering intensity contribution from the matrix ion (c.f. Figure 6(a)).

The intensity distribution of these ions observed with ion mobility is typical of distributions for endogenous species. The image of the interfering matrix ion is similar with and without IMS separation, as the intensity contribution made by the 402.019 Da ion was very limited. This can be seen by comparing Figures 6(b) and 9(b).

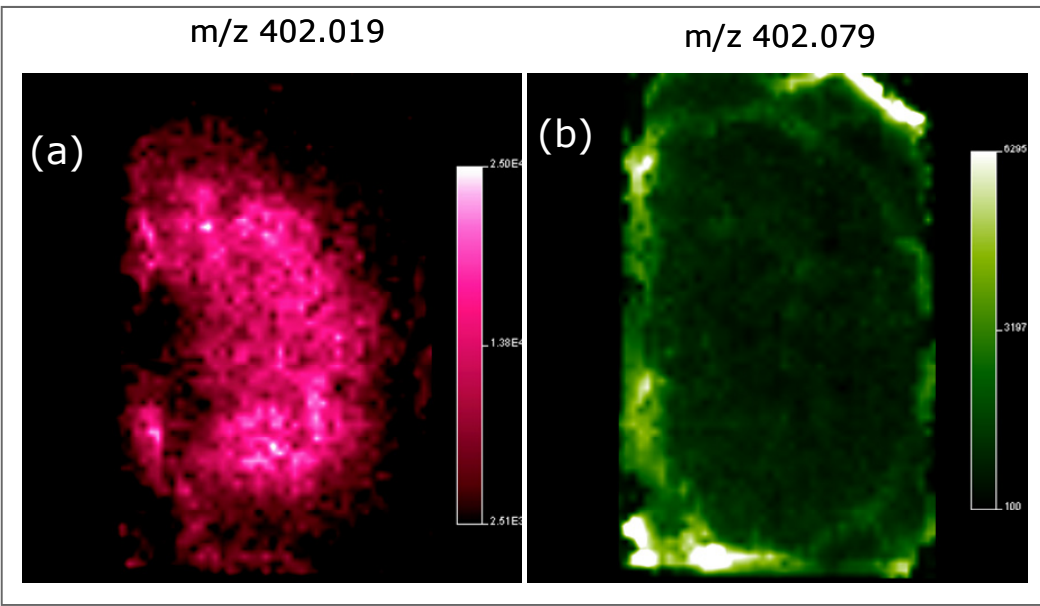


Figure 9. (a) Ion image of  $m/z$  402.019 with IMS (2.7 ms – 3.3 ms) and (b) image of  $m/z$  402.079 (interfering background ion), with IMS (3.4 ms – 4.1 ms).

## CONCLUSION

- The combination of high efficiency ion mobility separation with MALDI provides a unique separation dimension to further enhance mass spectrometric imaging.
- Through the use of ion mobility separation isobaric species desorbed from tissue can be separated.
- IMS can be used to produce images without interference from background ions of similar mass. This can remove ambiguity from imaging experiments and lead to more precise localisation of the compound of interest, e.g. drugs and metabolites.
- HDMS has the potential to reduce the complexity and improve confidence in imaging experiments.

### References

1. K. Giles, S. Pringle, K. Worthington, D. Little, J. Wildgoose, R. Bateman, *Rapid Commun. Mass Spectrom.*, **2004**; 18: 2401-2414

